



Filtering multiphoton emission from state-of-the-art cavity quantum electrodynamics

CARLOS SÁNCHEZ MUÑOZ,^{1,6} FABRICE P. LAUSSY,^{2,3} ELENA DEL VALLE,⁴ CARLOS TEJEDOR,⁴
AND ALEJANDRO GONZÁLEZ-TUDELA^{5,*}

¹CEMS, RIKEN, Wako-shi, Saitama 351-0198, Japan

²Faculty of Science and Engineering, University of Wolverhampton, Wulfruna St, WV1 1LY, UK

³Russian Quantum Center, Novaya 100, 143025 Skolkovo, Moscow Region, Russia

⁴Departamento de Física Teórica de la Materia Condensada and Condensed Matter Physics Center (IFIMAC), Facultad de Ciencias, Universidad Autónoma de Madrid, E-28049 Madrid, Spain

⁵Max-Planck Institut für Quantenoptik, Hans-Kopfermann-Strasse 1, 85748 Garching, Germany

⁶e-mail: carlossmwolff@gmail.com

*Corresponding author: alejandro.gonzalez-tudela@mpq.mpg.de

Received 9 August 2017; revised 24 October 2017; accepted 31 October 2017 (Doc. ID 304578); published 8 January 2018

Engineering multiphoton states is an outstanding challenge with applications in multiple fields such as quantum metrology, quantum lithography, or even biological sensing. State-of-the-art methods to obtain them rely on post-selection, multi-level systems, or Rydberg atomic ensembles. Recently, it was shown that a strongly driven two-level system interacting with a detuned cavity mode can be engineered to continuously emit n -photon states. In the present work, we show that spectral filtering of its emission relaxes considerably the requirements on the system parameters even to the more accessible *bad-cavity* situation, opening up the possibility of implementing this protocol in a much wider landscape of different platforms. This improvement is based on a key observation: in the imperfect case where only a certain fraction of emission is composed of n -photon states, these have a well-defined energy separated from the rest of the signal, which allows one to reveal and purify multiphoton emission just by frequency filtering. We demonstrate these results by obtaining analytical expressions for the relevant figures of merit of multiphoton emission, such as the n -photon coupling rate between cavity and emitter, the fraction of light emitted as n -photon states, and n -photon emission rates. This allows us to make a systematic study of such figures of merit as a function of the system parameters and demonstrate the viability of the protocol in several relevant types of cavity quantum electrodynamics setups, where we take into account the impact of their respective experimental limitations. © 2018 Optical Society of America

OCIS codes: (270.0270) Quantum optics; (270.4180) Multiphoton processes.

<https://doi.org/10.1364/OPTICA.5.000014>

1. INTRODUCTION

Non-classical states of light are a fundamental ingredient in the development of photonic quantum technologies such as quantum communication [1], quantum metrology [2], lithography [3], spectroscopy [4,5], or biological sensing [6,7]. The generation of single photons is experimentally accessible by several methods, such as exploiting the single-photon nonlinearity of natural and artificial atoms [8–14] or using correlated photon pairs in nonlinear crystals [15] or biexciton states [16–18]. However, obtaining multiphoton states is a much more challenging task, as the n -photon interactions are generally very weak. Current methods to generate multiphoton states in the optical regime are mostly probabilistic and rely on using single photons, linear optics, and post-selection to build up higher photon numbers. Unfortunately, they suffer from an exponential scaling of success with increasing photon number [19]. Thus, it is still of

fundamental and practical interest to search for novel mechanisms to engineer light at the n -photon level.

With this motivation, several methods have been proposed to generate n -photon states in very different scenarios, such as Rydberg atomic ensembles [20–22], atoms coupled to waveguide systems [23–25], or using multilevel atoms [26–30] or cavity quantum electrodynamics (QED) setups [31,32]. Particularly appealing, due to its simplicity, is the proposal in Ref. [32], which requires a single coherently driven two-level system (2LS), with driving amplitude Ω , coupled to a single cavity mode with strength g . In the limit, i.e., $\Omega \gg g$, it was shown that by appropriately placing the cavity resonance, the system can be brought to emit n -photon states (termed as n -photon bundles). However, the broadening introduced by the cavity and 2LS losses, denoted as γ_a/σ , respectively, also leads to the emission of photons that are not released in the form of n -photon bundles, and therefore

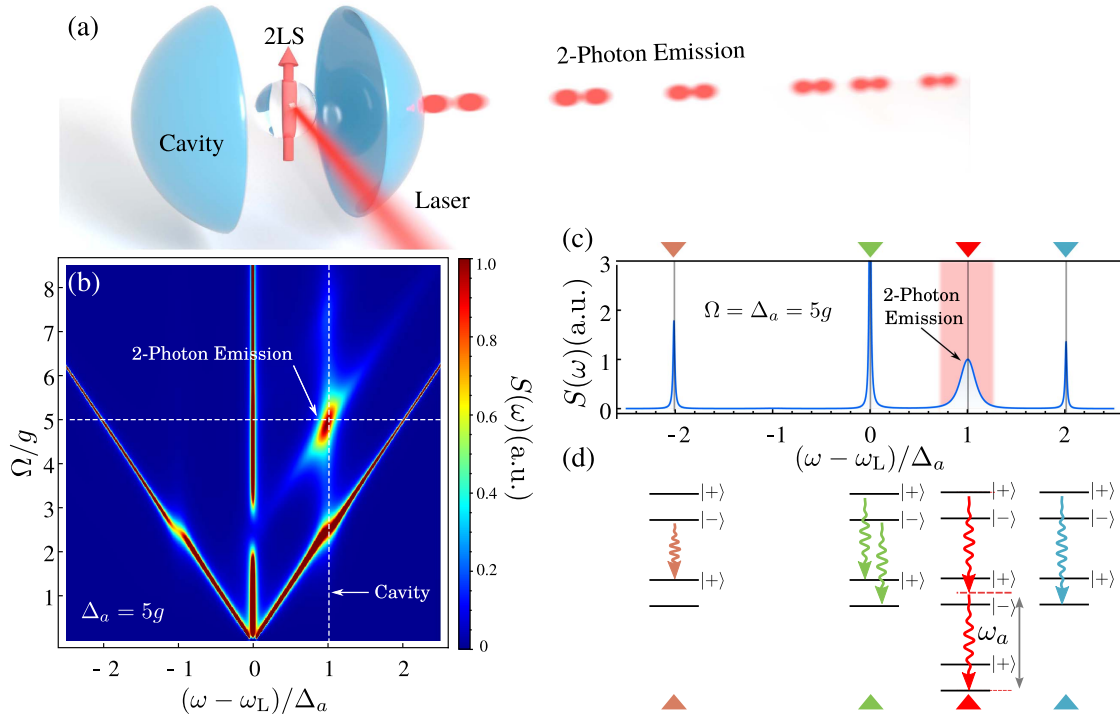


Fig. 1. (a) Scheme of the proposed setup: a two-level system is coupled to a cavity and strongly driven by a classical field. By selecting the proper cavity frequency, the system emits a continuous stream of photon pairs. (b) Evidence of two-photon emission in the cavity emission spectrum, plotted as a function of the driving field amplitude. The driving laser is in resonance with the 2LS, and the cavity is detuned by $\Delta_a = 5g$. Mollow sidebands appear in the spectrum at $\omega = \omega_L \pm 2\Omega$. When the cavity frequency lies between a sideband and the central peak, $\Delta_a = \pm\Omega$, two-photon emission is seen as a clear feature in the spectrum. At higher pumping one can also observe a small feature related to the three-photon resonance when Ω is such that $\Delta_a = \Delta_a^{(3)} = 2\Omega/2$, though it is weak because the experimental parameters are not good enough. (c) Spectrum in the regime of two-photon emission at $\Omega = \Delta_a$. (d) Transitions in the ladder of dressed states giving rise to the four peaks featured in panel (c). Simulation parameters: $\gamma_a = 1.3g$, $\gamma_\sigma = 0.01g$.

contaminate the n -photon character of the output field. In order to obtain emission with a large fraction of n -photon states, which defines the *purity* of n -photon emission [32], the coupling rate between the cavity and 2LS was taken in the strong coupling regime with $g > \gamma_{a,\sigma}$.

Here, we revisit this proposal to obtain analytical expressions for the figures of merit of the mechanism, such as the n -photon couplings, efficiency rates, and the purity of n -photon emission. Moreover, we identify the spectral distribution of both the spurious and the n -photon component of the cavity emission. In particular, we show that they are emitted in different frequency windows, such that the contaminating photons can be mostly suppressed with appropriate frequency filtering. This simple insight leads to better figures of merit for the n -photon emission and lifts the strong coupling requirements to observe such effects. In the particular case of two-photon emission, we show how high purities can be obtained as long as the rate of emission into the cavity with respect to free space, i.e., the cooperativity $C = 4g^2/(\gamma_a\gamma_\sigma)$, is large (the so-called *bad-cavity* limit). This opens up the possibility of implementing this proposal in a wide variety of platforms, such as semiconductor quantum dots (QDs) [33–36] or atom-nanophotonics [37,38], where the bad-cavity limit has been observed, but the strong coupling condition is hard to obtain. Another consequence of the spectral isolation of n -photon bundles is that they manifest as a clear feature in the spectrum, offering the simplest smoking gun to experimentally evidence n -photon emission (see Fig. 1).

The outline of the paper reads as follows: in Section 2 we review the setup and the mechanism proposed in Ref. [32] and derive analytical expressions for the figures of merit of n -photon emission, allowing us to show clearly how these depend on the system parameters. Then, in Section 3, we show the spectral distribution of the cavity emission in the n -photon resonance configuration and characterize the improvement in the figures of merit when filtering out the uncorrelated photons. In Section 4, we analyze several experimental limitations of the platforms where our proposal can be implemented, such as semiconductor or atomic cavity QED, and study their impact on the figures of merit for n -photon emission. Finally, we summarize our findings and point to future directions of work in Section 5.

2. SYSTEM AND GENERAL MECHANISM

The proposal in Ref. [32] is based on two cornerstones of quantum optics, namely, resonance fluorescence [39] and cavity QED [40,41]. In particular, it requires a single 2LS interacting both with a classical field, with amplitude Ω , and a quantum one, most simply implemented by a single-mode cavity coupled to the 2LS with strength g [see Fig. 1(a)]. For simplicity, we assume that the laser frequency, ω_L , is resonant with the transition frequency of the 2LS, ω_σ , as it makes the analysis simpler, at the expense of only weakly worsening the efficiency. Besides, the system is operated in the dispersive regime, where the 2LS and cavity are detuned. In this configuration, strong correlations can be

sustained between them even if their coupling is closer to a weak-coupling scenario with a small admixture of the bare states [42]. In these conditions, the total Hamiltonian of the combined system reads (using $\hbar = 1$)

$$H = \Delta_a a^\dagger a + g(a^\dagger \sigma + \sigma^\dagger a) + \Omega(\sigma + \sigma^\dagger), \quad (1)$$

which we have written in a frame rotating with the laser/2LS frequency to make it time independent, such that $\Delta_a = \omega_a - \omega_\sigma$ is the cavity-2LS detuning. The operators a^\dagger/a (σ^\dagger/σ) represent the creation/annihilation operators of the cavity (2LS) system. To take into account the cavity and 2LS losses, the Hamiltonian picture must be upgraded to a master equation description that takes into account the coupling to external baths. This results in an effective master equation that can be written

$$\frac{d\rho}{dt} = -i[H, \rho] + \frac{\gamma_\sigma}{2} \mathcal{L}_\sigma[\rho] + \frac{\gamma_a}{2} \mathcal{L}_a[\rho], \quad (2)$$

where $\mathcal{L}_O[\rho] \equiv 2O\rho O^\dagger - O^\dagger O\rho - \rho O^\dagger O$ is a Lindblad term describing the leakage of photons from both the cavity and the bare 2LS.

When $g = 0$, we recover the standard resonance fluorescence situation. This configuration has been traditionally exploited in the weak driving limit, $\Omega \ll \gamma_\sigma$, to generate individual single photons [10–13] emitted within a small spectral window around the 2LS frequency. In the strong driving limit, $\Omega \gg \gamma_\sigma$, the classical field dresses the 2LS levels, leading to two new eigenstates of the system, $|\pm\rangle = \frac{1}{\sqrt{2}}(|g\rangle \pm |e\rangle)$, with eigenenergies $E_\pm = \omega_\sigma \pm \Omega$. These dressed states deform the incoherent spectrum of 2LS from a single peak to the well-known Mollow triplet [39]. This spectral shape can be easily understood from single photon transitions in the dressed state picture [43] [see Fig. 1(d)], corresponding to $|\pm\rangle \rightarrow |\pm\rangle$ and $|\mp\rangle \rightarrow |\pm\rangle$, which explains why three peaks appear at frequencies $\omega_\sigma(\pm 2\Omega)$. Something that generally goes unnoticed is that, in the strong driving limit, the 2LS also provides nonlinearities at the multiphoton level. These nonlinearities can be understood as n -photon transitions in the ladder of dressed states, going from a state $|\pm\rangle$ to a state $|\mp\rangle$, n rungs below. As illustrated for the case $n = 2$ in Fig. 1(d), these processes are out of resonance from the first-order transitions associated to the Mollow triplet, and, for the case of photons of equal energy, it is easy to see that their energy is $\pm 2\Omega/n$. These multiphoton transitions are typically hidden by the single-photon processes, as they are of smaller order. However, they can be made visible, e.g., by using frequency-resolved correlations [44,45], as recently observed in experiments [46,47]. Remarkably, these correlations in frequency space are strong enough to violate classical inequalities [46,48].

Unfortunately, the emission of these strongly correlated photons is scarce and, therefore, difficult to exploit. An alternative and powerful way of capitalizing on these photons consists of coupling the strongly driven 2LS to a cavity (making $g \neq 0$ in our model) and setting the cavity energy exactly at these multiphoton resonances, $\Delta_a^{(n)} = \pm 2\Omega/n$. Using that simple prescription, it was shown by using a quantum jump simulation [32] that one is able to Purcell-enhance the n -th photon process with respect to the single-photon ones, leading to (almost) perfect emission in groups or *bundles* of photons.

Figure 1 illustrates this effect for the case of $n = 2$ photons. In particular, in panel (b) we show the evolution of the incoherent part of the cavity spectrum, $S(\omega) \propto \lim_{t \rightarrow \infty} \int d\tau \langle a^\dagger(t) a$

$(t + \tau) \rangle e^{i\omega\tau}$, with increasing driving Ω for a fixed cavity-2LS detuning of $\Delta_a = 5g$, also with $\gamma_a = 1.3g$ and $\gamma_\sigma = 0.01$, such that $C \sim 300$. These parameters are similar to those reported in experimental works that have already performed measurements similar to what we show in Fig. 1(b) [49,50]. The main difference between those measurements and what we show here lies in the range of Ω considered, which in such experiments was not taken to the values where the new effects that we report clearly manifest themselves. We can distinguish three different regimes:

- When the driving is small, we only observe a single peak at the 2LS frequency. The main effect of the cavity here is to renormalize the broadening of such a peak to $\sim \gamma_\sigma + \frac{4g^2\gamma_a}{4\Delta_a^2 + \gamma_a^2}$, that is, the sum of the individual 2LS decay plus the broadening provided by the cavity emission.
- As the driving increases, the cavity spectrum $S(\omega)$ starts to display a triplet structure that is distorted by the finite detuning, Δ_a , as it breaks the symmetry between the upper/lower sidebands from the bare Mollow triplet. Interestingly, when Ω is such that Δ_a is resonant with the upper sideband, i.e., $\Delta_a^{(1)} = 2\Omega = 5g$, one observes a strong suppression of the central peak and a very strong asymmetry between the two sidebands.

The origin of these features can be traced back to the natural tendency of the photons emitted from strongly driven 2LSs, which preferentially emit cascaded photons between the different sidebands rather than from the sideband and the central peaks, as evidenced by the cross-correlations between the peaks [45,48,51]. These preferences can also translate into features in the cavity spectrum, as shown in Ref. [27]. In our particular case, when we place the cavity resonant with one of the sidebands, it Purcell-enhances the cascaded emission between different sidebands, while strongly suppressing the central peak one, as shown in Fig. 1(b).

- The most interesting regime for this paper occurs when Ω is such that $\Delta_a = \Delta_a^{(2)} = \Omega = 5g$. Around this value of Ω , we observe in Fig. 1(b) the appearance of an extra peak in the cavity spectrum, which is precisely the one that generates the photon pairs predicted in Ref. [32]. To make it more clear, we plot a horizontal cut at $\Omega = 5g$ in Fig. 1(c). The four peaks can be easily identified with processes in the dressed state picture, as schematically depicted in Fig. 1(d): on the one hand, we observe the conventional single-photon processes at $\omega_\sigma - 2\Omega$, ω_σ and $\omega_\sigma + 2\Omega$; on the other hand, at the cavity frequency, between the central peak and the upper sideband, we observe a peak that corresponds to the cascaded emission of two photons at frequencies $\omega_\sigma + \Omega$. This peak is broader than the others due to the Purcell enhancement by the cavity.

The two-photon physics is still apparent even when one is not exactly at the two-photon resonance. Namely, the spectrum of Fig. 1(b) features a diagonal line that crosses the two-photons resonance peak. This can be understood as the Purcell-enhancement of a two-photon transition in which the photons do not have the same frequency, but their sum fulfills $\Delta_1 + \Delta_2 = 2\Omega$. When these two frequencies are not too distinct, the cavity is able to Purcell-enhance the emission of a photon at its own resonance frequency, Δ_a , and a second photon at a frequency $\Delta_2 = 2\Omega - \Delta_a$, which defines the line observed in the plot.

At higher pumpings, i.e., $\Omega = 3\Delta_a/2 = 7.5g$, one should observe the enhancement attributed to the three-photon resonance. Although dim, this feature is visible even in Fig. 1(b), despite that we did not use the best parameters available in state-of-the-art cavity QED.

To certify that one is dealing with true n -photon emission, one can study the statistics of the output field, as shown in Refs. [27,28,32]. However, in this paper we will use the appearance of these extra peaks in $S(\omega)$ as the signature for n -photon emission, as it is the simplest experimentally relevant smoking gun for multiphoton emission. A similar method has been used, for instance, to experimentally evidence Purcell-enhanced two-photon emission in a biexcitonic radiative cascade [52].

A. Analytical Derivation of the n -Photon Coupling Rate

After having illustrated the mechanism for a particular situation, one of the main goals of this paper is to gain analytical understanding on the figures of merit of the emission. As shown in Fig. 1(c), all the nonlinear processes appearing in $S(\omega)$ are well understood in the dressed state picture. Thus, it is enlightening to write the Hamiltonian in the dressed state basis, where it reads

$$H = \Omega \tilde{\sigma}_z + \Delta_a a^\dagger a + \frac{g}{2} \{a^\dagger (\tilde{\sigma} - \tilde{\sigma}^\dagger + \tilde{\sigma}_z) + \text{h.c.}\}, \quad (3)$$

where $\tilde{\sigma} = |- \rangle \langle + |$ and $\tilde{\sigma}_z = | + \rangle \langle + | - | - \rangle \langle - |$. In the strong driving limit, $\Omega \gg g$, and when the cavity is close to the n -th photon resonance, i.e., $\Delta_a \approx \Delta_a^{(n)}$, the energy levels of the Hamiltonian are structured in manifolds $\mathcal{E}_{m,n} = \{|+, m\rangle, |- , m+n\rangle\}$ (where m is the number of photons in the cavity) such that the energy separation between levels inside a manifold is much smaller than the energy separation between different manifolds. This energy separation allows one to perform an adiabatic elimination of the fast degrees of freedom to construct an effective Hamiltonian that does not couple the manifolds between them. Under these conditions, the dynamics can then be described by an effective n -photon coupling Hamiltonian,

$$H_{\text{eff}}^{(n)} = \Omega \tilde{\sigma}_z + \Delta_a a^\dagger a + g^{(n)} (\tilde{\sigma}^\dagger a^n + \tilde{\sigma} a^{\dagger n}), \quad (4)$$

which generates n -photon Rabi oscillations between the states $|+, m\rangle$ and $|- , m+n\rangle$ with rate (see Supplement 1.1 for derivation)

$$g^{(n)} = \frac{g^n}{2(n-1)!^2} \left(\frac{n^2}{4\Omega} \right)^{n-1}. \quad (5)$$

There are also small energy shifts of the bare 2LS and cavity energies that move the n -photon resonance from the values $\Delta_a^{(n)} = \pm 2R/n$. For simplicity, we will omit writing these shifts in the following discussions, but include them consistently to perform the calculations.

Performing the same change of basis into the 2LS Lindblad operators, we arrive at

$$\frac{\gamma_\sigma}{2} \mathcal{L}_\sigma[\rho] \approx \left(\frac{\gamma_\sigma}{8} \mathcal{L}_{\tilde{\sigma}} + \frac{\gamma_\sigma}{8} \mathcal{L}_{\tilde{\sigma}^\dagger} + \frac{\gamma_\sigma}{2} \mathcal{L}_{\tilde{\sigma}^\dagger \tilde{\sigma}} \right) [\rho], \quad (6)$$

where other fast-rotating terms are eliminated under the assumption $\Omega \gg \gamma_\sigma$. Therefore, the bare 2LS decay transforms, in the dressed state basis, into: (i) an effective decay rate $\gamma_{\tilde{\sigma}} = \frac{\gamma_\sigma}{4}$; (ii) an effective pumping rate $P_{\tilde{\sigma}} = \frac{\gamma_\sigma}{4}$; and (iii) a dephasing term with rate $\gamma_{\tilde{\phi}} = \gamma_\sigma$.

By solving the master equation with the n -photon Hamiltonian in the dressed basis,

$$\begin{aligned} \frac{d\rho}{dt} = & -i[H_{\text{eff}}^{(n)}, \rho] + \frac{\gamma_a}{2} \mathcal{L}_a[\rho] + \frac{\gamma_{\tilde{\sigma}}}{2} \mathcal{L}_{\tilde{\sigma}}[\rho] \\ & + \frac{P_{\tilde{\sigma}}}{2} \mathcal{L}_{\tilde{\sigma}^\dagger}[\rho] + \frac{\gamma_{\tilde{\phi}}}{2} \mathcal{L}_{\tilde{\sigma}^\dagger \tilde{\sigma}}[\rho], \end{aligned} \quad (7)$$

we calculate the amount of cavity population introduced via the n -photon coupling of Eq. (4) under the assumption $g^{(n)} \ll \gamma_a$, obtaining (see Supplement 1.2)

$$n_a^{(n)} \approx n^2 \frac{\kappa^{(n)}}{\Gamma_{\tilde{\sigma}}(n\gamma_a + \Gamma_{\tilde{\sigma}} + \gamma_{\tilde{\phi}}) + \kappa^{(n)}n\gamma_a} P_{\tilde{\sigma}}, \quad (8)$$

where $\Gamma_{\tilde{\sigma}} = \gamma_{\tilde{\sigma}} + P_{\tilde{\sigma}}$, and $\kappa^{(n)} = \frac{4(n-1)!(g^{(n)})^2}{\gamma_a}$ is a generalized n -photon Purcell rate. In the limit $n\gamma_a \gg \gamma_\sigma$, the previous expression simplifies to

$$n_a^{(n)} \approx n \frac{\kappa^{(n)}}{\gamma_a} \frac{P_{\tilde{\sigma}}}{\kappa^{(n)} + \Gamma_{\tilde{\sigma}}}, \quad (9)$$

in which each term has a transparent meaning: (i) the term $\frac{P_{\tilde{\sigma}}}{\kappa^{(n)} + \Gamma_{\tilde{\sigma}}}$ is the population of the dressed 2LS that mediates the n -photon coupling; (ii) the term $\frac{\kappa^{(n)}}{\gamma_a}$ is the ratio between the effective pumping to the cavity mode through the n -photon Purcell decay rate, $\kappa^{(n)}$, and the cavity decay rate, γ_a ; (iii) the factor n takes into account that every time a jump occurs in the effective dressed 2LS, n photons are introduced in the cavity. One can confirm, by looking at the output field of the cavity, that these photons which are introduced through the cavity in groups of n , are also emitted as such, as was established in Ref. [27,32]. The timescale between the n -photon states is $\sim (\kappa^{(n)} + \gamma_{\tilde{\sigma}})^{-1}$, as it is the time it takes to reload the dressed 2LS after an n -photon quantum jump. The spectral width of the n -photon wavepacket is of the order of $n\gamma_a$. Thus, in order to obtain antibunched n -photon emission, it must be satisfied that [28] $n\gamma_a \gg \kappa^{(n)} + \gamma_{\tilde{\sigma}}$.

However, it was shown [32] that even in the perfect resonant case the n -photon emission at the output of the cavity field is always contaminated by the emission of uncorrelated single-photon states. The origin of such photons is that, when writing the effective Hamiltonian of Eq. (4), we are neglecting the off-resonant, but first-order, processes that also generate population in the cavity, which we denote by $n_a^{(1)}$. These processes are especially relevant when the broadening introduced by $\gamma_{a,\sigma}$ is considerable. Interestingly, this off-resonant population $n_a^{(1)}$ can also be analytically estimated in the limit $\Omega \gg g$. For example, for the two-photon resonant situation that we will be focusing on along this paper, $\Delta_a = \Delta_a^{(2)}$, and in the limit of $\gamma_\sigma \ll \Omega$, $\Delta_a \gamma_a$, it can be approximated by (see Supplement 1.2)

$$\begin{aligned} n_a^{(1)} \approx & \frac{2g^2(\gamma_a^2 + 28\Omega^2)}{(\gamma_a^2 + 4\Omega^2)(\gamma_a^2 + 36\Omega^2)} \\ & + \frac{32g^2\Omega^2(\gamma_a^4 + 432\Omega^4)\gamma_{\tilde{\sigma}}}{\gamma_a(\gamma_a^2 + 4\Omega^2)^2(\gamma_a^2 + 36\Omega^2)^2}. \end{aligned} \quad (10)$$

The more general expression as a function of Δ_a can be found in the Supplement 1. Finally, we make the assumption that the total population in the cavity is given by the sum of the two mechanisms described above, $n_a \approx n_a^{(1)} + n_a^{(n)}$. We numerically confirmed this is a good assumption in the regime of validity of the approximations, that is, $\Omega \gg g$, $\gamma_\sigma \ll \Omega$, $\Delta_a \gamma_a$ and $g^{(n)} \ll \gamma_a$, as numerically confirmed in Fig. 2 (see discussion below).

B. Characterizing n -Photon Emission

Thanks to the analytical results that we developed in the previous section, we can make a more systematic analysis of the main figures of merit of the n -photon emission of our proposal, namely,

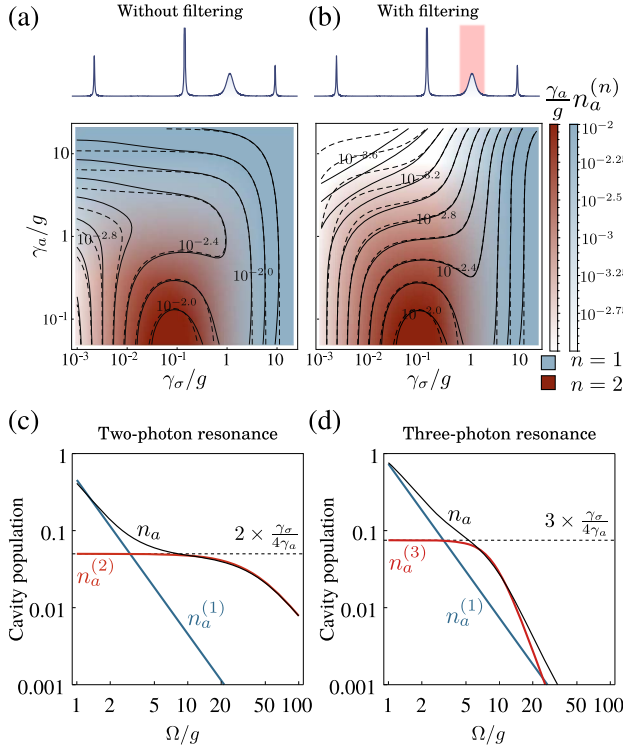


Fig. 2. (a) Joint plot of two-photon [$n_a^{(2)}$, red] and one-photon [$n_a^{(1)}$, blue] emission rates as a function of cavity (γ_a) and 2LS (γ_σ) decay rates. Contour lines correspond to the total population n_a computed numerically (solid) and analytically (dashed), based on the assumption $n_a \approx n_a^{(2)} + n_a^{(1)}$, and using the analytical approximations of Eqs. (8) and of Eq. (10) to analytically calculate the populations $n_a^{(n)}$ and $n_a^{(1)}$, respectively. (b) Two-photon emission rate [$n_a^{(2)}$, red] and one-photon emission rate [$n_a^{(1)}$, blue] at the cavity frequency. Contour lines correspond to the total filtered emission $n_{a,f}$, computed numerically (solid) and analytically, based on the assumption $n_{a,f} \approx n_a^{(2)} + n_a^{(1)}$ and Eqs. (8) and (23). $\Omega = 20g$ in panels (a) and (b). (c) Components of the cavity population as a function of Ω when the cavity is fixed at the two-photon resonance ($\Delta_a = \Omega$). Black: total cavity population. Blue: single-photon component of cavity population as given in Eq. (10). Red: two-photon component of cavity population $n_a^{(2)}$ as given by Eq. (8). Dashed, horizontal lines mark the weak driving limit of $n_a^{(n)}$ given by Eq. (13). (d) Same as in (c), for the three-photon resonance. Simulation parameters: $\gamma_a = 0.1g$ and $\gamma_\sigma = 0.01g$.

(i) the n -photon emission rate through the cavity mode that is given by $\gamma_a n_a^{(n)}$; and (ii) the *purity of n -photon emission*, defined as the fraction of the total population that is given by the n -photon population,

$$\pi_n = \frac{n_a^{(n)}}{n_a} \approx \frac{n_a^{(n)}}{n_a^{(1)} + n_a^{(n)}}. \quad (11)$$

We start by showing a contour plot in Fig. 2(a) of the single (in blue) and two-photon (in red) emission rates as a function of $(\gamma_a, \gamma_\sigma)/g$ for a situation with $\Omega = 20g$ and Δ_a tuned to the two-photon resonance, i.e., $\Delta = \Delta_a^{(2)} = \Omega$. Both plots are superimposed to facilitate the comparison. We confirm that, in order for the two-photon process to dominate, it is required that $\gamma_{a,\sigma} < g$, which corresponds to the red region in the lower part of the figure. This was the regime considered in Ref. [32]. As γ_a increases, the importance of the n -photon emission rate also

decreases, as expected from the analytical formula of $n_a^{(n)}$ in Eq. (9) since $\kappa^{(n)} \propto 1/\gamma_a$. The behavior with γ_σ is, however, less trivial, as there is a trade-off between increasing the pumping of the effective two-level system, $P_{\bar{\sigma}} \propto \gamma_\sigma$, but at the same time increasing its losses $\gamma_{\bar{\sigma}}$, which results in an optimal γ_σ as shown in Fig. 2(a). As we have the analytical expressions for $n_a^{(n)}$, we can find the optimal $\gamma_\sigma^{n,\text{opt}}$, defined as the one which gives the largest amount of $n_a^{(n)}$ for a fixed set of parameters. The general expression for any n reads

$$\gamma_\sigma^{(n,\text{opt})} = \left(\frac{gn^2}{4\Omega} \right)^n \frac{8\Omega}{\sqrt{3(n!)^3}}. \quad (12)$$

For the case $n = 2$ that we plot in Fig. 2(a), the optimal decay is obtained when $\gamma_\sigma^{(2,\text{opt})} = 2\sqrt{2/3}g^2/\Omega \approx 0.08g$, which coincides with the numerical results shown in that figure.

Another interesting characteristic to explore is the dependence of the efficiencies with Ω , as this is an experimentally tunable parameter. In Figs. 2(c)–2(d) we plot the dependence with Ω of the total cavity population (black), and its single (blue) and n -photon (red) components given by Eqs. (10) and (8), for a system that is fixed at the two- to three-photon resonance, respectively, i.e., $\Delta_a = \Delta_a^{(2-3)}$. This means that we change Δ_a accordingly as the driving increases. There are several interesting conclusions to be extracted from this figure:

- In both the two- and three-photon resonance situations, the analytical formulas capture very well, both qualitatively and quantitatively, the full numerical results in all the regimes of Ω depicted in Figs. 2(c)–2(d).

- As expected at weak drivings, the single-photon population, $n_a^{(1)}$, dominates over the n -photon one, as the detuning is not enough to suppress one-photon processes. From the formula of $n_a^{(n)}$, one can actually obtain a simple formula for the limit of very weak driving,

$$n_a^{(n)} \approx \frac{n\gamma_\sigma}{4\gamma_a}, \quad (\Omega \rightarrow 0), \quad (13)$$

which is the horizontal line that we plot in Figs. 2(c)–2(d).

- As the driving increases, both $n_a^{(1)}$ and $n_a^{(n)}$ (and therefore n_a) decrease, but with a significant difference between the two- and the three-photon situation. At the two-photon resonant case, $n_a^{(1)}$ and $n_a^{(2)}$ decrease with the same scaling with Ω , which allows $n_a^{(2)}$ to dominate even for very large Ω . On the contrary, in the case of three photons, $n_a^{(3)}$ decreases faster than $n_a^{(1)}$ such that there will be an optimal Ω to maximize $n_a^{(3)}$ over $n_a^{(1)}$. This behavior can also be obtained with the analytical formulas by expanding them in the $\Omega \rightarrow \infty$ limit,

$$n_a^{(n)} \approx \frac{g^{2n}}{\Omega^{2(n-1)}} A_n \propto \frac{1}{\Omega^{2(n-1)}}, \quad (14)$$

$$n_a^{(1)} \approx \left(\frac{g^2}{\Omega^2} \right) \frac{n^3(2+n^2)\gamma_\sigma + n(n^4 - n^2 + 2)\gamma_a}{16(n^2 - 1)^2\gamma_a} \propto \frac{1}{\Omega^2}, \quad (15)$$

where A_n reads,

$$A_n = [16^{n-1}\gamma_a(2n\gamma_a + 3\gamma_\sigma)n^{2(1-2n)}(n-1)!^3]^{-1}. \quad (16)$$

The convergence to that limit is obtained when $(\Omega/g)^{2(n-1)} \gg C$ [$\Omega \gg \gamma_{a,\sigma}$] for $n_a^{(n)}$ [$n_a^{(1)}$], which are the limits in which these formulas are valid.

From this discussion, we observe that there is a non-trivial trade-off between absolute multiphoton emission rates and the

purity of the multiphoton source as defined in Eq. (11). Using the analytical expressions we developed, we can find an approximated formula for the π_n that reads,

$$\pi_n \approx \left\{ 1 + \left[\frac{4g(\gamma_a^2 + 28\Omega^2)}{(\gamma_a^2 + 4\Omega^2)(\gamma_a^2 + 36\Omega^2)} + \frac{32g^2\Omega^2(\gamma_a^4 + 432\Omega^4)\gamma_\sigma}{\gamma_a(\gamma_a^2 + 4\Omega^2)^2(\gamma_a^2 + 36\Omega^2)^2} \right] \times \left[\frac{4\gamma_a}{n\gamma_\sigma} + \frac{\Omega^{2(n-1)}}{g^{2n}A_n} \right] \right\}^{-1}. \quad (17)$$

We numerically checked (see [Supplement 1](#)) that the π_n obtained from the analytical formulas agree quantitatively well with the ones that can be obtained from the photon counting distribution of the output field [53], as was introduced in Refs. [27,32].

One can now use Eq. (17) to obtain simple asymptotic expressions. For example, in the large driving limit defined above, one obtains the following formula for the purity of two-photon emission:

$$\pi_2 \approx \left(1 + \frac{7}{18} \frac{\gamma_a^2}{g^2} + \frac{8}{3C} + \frac{21}{18C} + \frac{8}{\gamma_a^2 C^2} \right)^{-1}, \quad (18)$$

where the term proportional to $(\gamma_a/g)^2$ evidences that one needs to have strong coupling parameters, $\gamma_a \ll g$, in order to obtain values of π_2 close to one, as was already observed in Ref. [32]. For values of n larger than 2, the asymptotic expression for the purity is $\pi_{n>2} \propto \frac{1}{\Omega^{2(n-1)}}$. This tells us that for the $n = 2$ case, one can always purify the two-photon emission by going to larger drivings, whereas for the $n > 2$ case, one has to find the optimal driving that maximizes the purity for a given set of parameters. The explanation for this is that $n_a^{(n)}$ is given, for $n = 1$, by an off-resonant, first-order process, and for $n > 1$, by a resonant, n -th order process. Only in the case of $n = 2$ these two properties (on-resonance and second-order) compensate and yield values of $n_a^{(2)}$ larger than $n_a^{(1)}$ at large drivings. Although in principle it is possible to find an optimal Ω for $n > 2$ by differentiating the expression of π_n , its expression is too cumbersome to write here. An alternative way to obtain an approximated optimal Ω consists in finding the point where the asymptotic expressions of $n_a^{(n)}$ at small and large driving cross. The latter procedure leads to a simple expression for the optimal driving, which reads,

$$\Omega_{\text{opt}}^{(n)} \approx \left(\frac{4\gamma_a g^{2n} A_n}{n\gamma_\sigma} \right)^{\frac{1}{2(n-1)}}. \quad (19)$$

We checked numerically that this is indeed a very good approximation by comparing with the exact numerical results. Finally, we want to note that for the particular case $n = 2$, we have observed that the cavity observable T , defined as

$$T \equiv \frac{2\langle a^{\dagger 2} a^2 \rangle}{\langle a^{\dagger} a \rangle}, \quad (20)$$

is a good approximation of π_2 under some circumstances, as shown in Fig. 5(a) (see [Supplement 1](#) for a more complete discussion). Note that this connection between the purity and T is not rigorous, since π_2 is a probability bounded by one by construction, and T is not. However, our results show that these two quantities show a similar enough behavior for T to be considered a valuable indicator of two-photon emission in the laboratory.

3. IMPROVEMENT BY FREQUENCY FILTERING

A. Spectral Distribution

As we have seen in Fig. 1, the multiphoton emission in our setup manifests as an extra peak in the incoherent cavity spectrum.

However, together with this extra peak, we still observe three other peaks reminiscent from the single-photon transitions of the Mollow triplet. A key observation is that the photons at these frequencies are the main origin of the small fraction of spurious photons that contaminate the multiphoton emission, which we labeled as $n_a^{(1)}$. The fact that these photons appear at frequencies well separated from the multiphoton peak allows one to purify the multiphoton source by frequency filtering, which has already been proven to be a way to optimize photon correlations in other situations [54,55]. Before analyzing the effect of the filtering, let us first show how to estimate the fraction of the total emission corresponding to each of the spectral peaks. Formally, the incoherent part of the cavity spectrum can be calculated in terms of the eigenvalues, λ_β , and eigenvectors of the Liouvillian of the system as follows [56,57]:

$$S(\omega) = \frac{1}{\pi} \sum_{\beta} \left[\frac{(\gamma_\beta/2)L_\beta}{(\omega - \omega_\beta)^2 + (\gamma_\beta/2)^2} - \frac{(\omega - \omega_\beta)K_\beta}{(\omega - \omega_\beta)^2 + (\gamma_\beta/2)^2} \right], \quad (21)$$

that is, a sum of Lorentzians centered at $\omega_\beta = \Re\{\lambda_\beta\}$ with line-width $\gamma_\beta = 2\Re\{\lambda_\beta\}$ (plus a dispersive part that takes into account possible interferences between them). The weights L_β, K_β are obtained from a combination of the eigenvectors of the Liouvillian and the steady state of ρ . It can be trivially shown that L_β satisfy that $n_a = \sum_{\beta} L_\beta$. Using that information, it is possible to estimate the amount of cavity population emitted at the frequency of the cavity, $n_{a,f}$, by summing those L_β whose corresponding ω_β is close to the cavity frequency,

$$n_{a,f} = \sum_{\omega_\beta \approx \omega_a} L_\beta. \quad (22)$$

We can now estimate the amount of light from the single-photon processes emitted at the cavity frequency, $n_{a,f}^{(1)}$, which is the one that we will not be able to get rid of by frequency filtering. This is done by using a similar analysis, but truncating the cavity's Hilbert space to one photon in order to exclude n -photon processes from the dynamics (see [Supplement 1.3](#)). The approximated expression for $n_{a,f}^{(1)}$ reads, in the limit of $\Omega \gg g, \gamma_a, \gamma_\sigma$,

$$n_{a,f}^{(1)} \approx \Re \left\{ \frac{32g^2(\gamma_a^2\Omega^2 + 4i\gamma_a\Delta_a\Omega^2 - 4\Delta_a^2\Omega^2 - 8\Omega^4)\gamma_\sigma}{\gamma_a(\gamma_a + 2i\Delta_a)^2(\gamma_a + 2i\Delta_a - 4i\Omega)^2(\gamma_a + 2i\Delta_a + 4i\Omega)^2} \right\}. \quad (23)$$

Interestingly, in the case of two-photon emission, this expression already appeared naturally in the formula we derived for $n_a^{(1)}$, since by substituting the two-photon condition $\Delta_a = \Delta_a^{(2)} = \Omega$ in Eq. (23), one obtains precisely the second term in the sum of Eq. (10). Therefore, we can now understand such a term as the fraction of cavity population grown by first-order processes that is emitted at the resonant cavity frequency. By comparing this quantity to the population of n -photon bundles $n_a^{(n)}$, we can obtain an estimate of the purity of multiphoton emission for the light filtered at the cavity frequency and determine to which extent the figures of merit of multiphoton emission are improved. The underlying assumption is that the single-photon peaks are separated enough such that a realistic filter can extract only the emission from the n -photon component.

B. Figures of Merit of the Filtered Emission

From the analysis made in the previous section, it is expected that by filtering out the cavity emission one can substantially improve the figures of merit of our multiphoton source. This is based on the assumption that only part of the undesired photons—with a population corresponding to $n_{a,f}^{(1)}$ —will be emitted at the cavity frequency, whereas the totality of the n -photon bundles are emitted at such frequency. We can confirm this assumption by applying the previous analysis to the Liouvillian of the master equation in Eq. (7) as shown in Fig. 3, where it is clearly seen how the two-photon population $n_a^{(2)}$ —computed from Eq. (7)—corresponds to the amount of the total population $n_{a,f}$ emitted at ω_a . This is a particular case in which all the photons emitted at the cavity frequency are two-photon bundles, and no spurious photons are emitted at that frequency. In a general situation, this could fail to be the case, which leads us to the definition of the *purity of filtered n -photon emission*, given by the fraction of the population emitted at the cavity frequency, which is composed by n -photon bundles,

$$\pi_n^f = \frac{n_a^{(n)}}{n_{a,f}}, \quad (24)$$

which in the case of two-photon emission can be approximated as $\pi_2^f \approx n_a^{(2)} / (n_{a,f}^{(1)} + n_a^{(2)})$. To illustrate the improvement brought by filtering, we show in Fig. 2(b) a contour plot of the emission rates $n_a^{(2)}$ (red) and $n_{a,f}^{(1)}$ (blue) as a function of $(\gamma_a, \gamma_\sigma)$ with the same $\Omega = 20g$ as the one used in Fig. 2(a). By comparing the two panels, we observe that the region in which the two-photon filtered emission dominates over the single-photon one is substantially enlarged with respect to the unfiltered situation, even including regions in the weak-coupling regime $\gamma_a/g < 1$. This is a major result, as it opens up the possibility of producing such multiphoton emission in systems within the bad-cavity limit, where $\gamma_{a,\sigma} < g$, but $C > 1$, which is commonplace in both cavity and waveguide QED in the optical regime [33,36–38].

Using the analytical formulas we derived in the previous section and Eq. (23) for $n_{a,f}^{(1)}$, we can obtain an asymptotic expression for the purity of n -photon filtered emission in the large driving limit, which for the two-photon case reads,

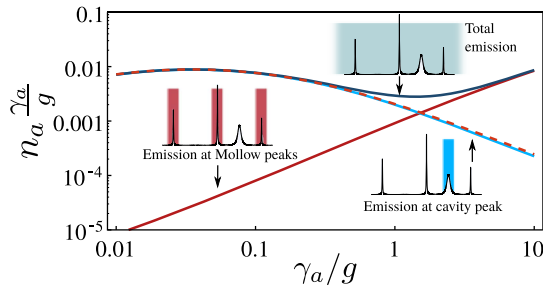


Fig. 3. Cavity emission rates at the two-photon resonance for three different spectral windows: central peak of the Mollow triplet (red), cavity peak (light blue), and total emission (dark blue). These rates have been numerically computed using Eq. (22). The bundle emission $\gamma_a n_a^{(2)}$ (dashed, orange) computed from the n -photon master equation given in Eq. (7) closely matches the emission at the cavity peak. This confirms that the light emitted at that frequency is composed of photon bundles, and that spurious emission can be eliminated by frequency filtering. Parameters: $\Omega/g = 20$ and $\gamma_\sigma/g = 0.025$.

$$\pi_2^f \approx \left(1 + \frac{8}{3C} + \frac{8g^2}{\gamma_a^2 C^2}\right)^{-1}. \quad (25)$$

By comparing this expression to Eq. (18), we can see clearly how frequency filtering allows us to get rid of the term proportional to $(\gamma_a/g)^2$ that enforces the strong coupling condition. Now, the limit $\gamma_a \gg g$ leaves us an expression for π_2^f that depends only on the cooperativity, $\pi_2^f \approx (1 + \frac{8}{3C})^{-1}$. This provides a simple way to evaluate the maximum purity that can be observed for a system with a given cooperativity without the need to perform demanding numerical calculations.

For the general case of n -photon emission with $n > 2$, the large driving limit of π_n^f goes as $\pi_n^f \propto \frac{1}{\Omega^{2(n-1)}}$. Even if this limit follows the same trend as in the unfiltered case, frequency filtering still provides a remarkable improvement in the figures of merit when an optimum driving is chosen. To illustrate it, we plot in Fig. 4(a) the filtered and unfiltered purity for the $n = 2, 3, 4$ photons situation as a function of γ_a/g for a system with $\Omega/g = 20$ and $\gamma_\sigma/g = 0.025, 0.005$ and 0.001 , respectively, where we observe a substantial improvement of the purity for all n . It is worth highlighting that 100% of n -photon emission is guaranteed for good-enough system parameters. Panel (b) depicts the underlying n -photon components of the cavity population, further corroborating our assumptions that the total population in the filtered and unfiltered cases can, in good approximation, be decomposed into components associated to n -photon processes. This plot, however, also shows an effect not discussed so far: the resonant n -photon emission can also be spoiled by other off-resonant multiphoton processes of lower-order $m < n$. In particular, we show that in the case of

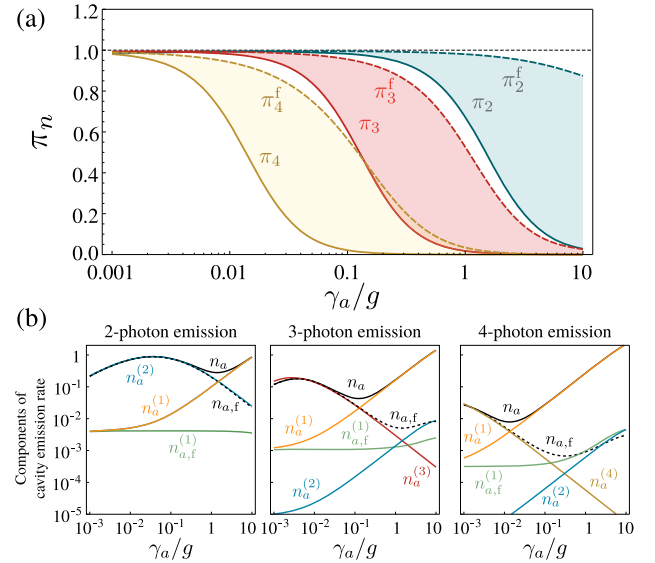


Fig. 4. (a) Numerical calculations for the purity of two-, three-, and four-photon emission for unfiltered (π_n , solid) and filtered (π_n^f , dashed) cases, given by Eq. (11) and Eq. (26), with $n_a^{(1)}$ and $n_{a,f}^{(1)}$ computed numerically from a model truncated at one photon, and with $n_a^{(n)}$ for $n \geq 2$ computed numerically from the master equation Eq. (7), where the effective n -photon coupling rates are given by the analytical expression of Eq. (5). Parameters: $\Omega/g = 20$, $\gamma_\sigma/g = 0.025, 0.005$, and 0.001 for $n = 2, 3, 4$, respectively. (b) Numerically computed unfiltered and filtered emission rates, $\gamma_a n_a$ (solid, black) and $\gamma_a n_{a,f}$ (dashed, black), compared to the underlying n -photon components of the cavity emission rate, $\gamma_a n_a^{(n)}$, used in the computation of π_n and π_n^f of panel (a).

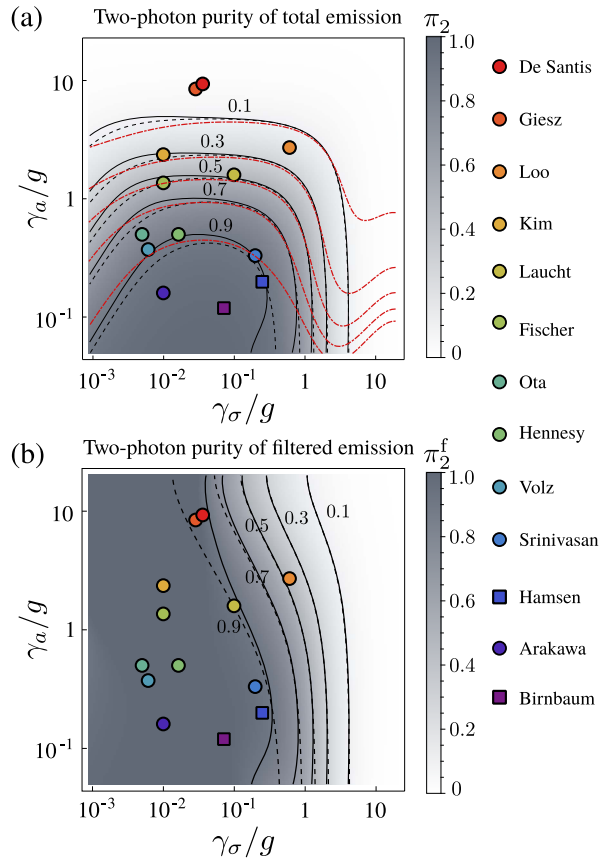


Fig. 5. Purity of two-photon emission in the unfiltered (a) and filtered (b) case, as a function of cavity decay rate γ_a and 2LS decay rate γ_σ . Colored points correspond to experimental state-of-the-art samples, with values summarized in Table 1. Circles correspond to semiconductor QDs, and squares correspond to atoms. In panel (a), the values of the observable T defined in Eq. (20) are shown in dashed-dotted red lines for comparison. Parameters: $\Omega = 20g$.

three- and four-photon emission, and for large values of γ_a , the population $n_a^{(2)}$ grown by the off-resonant two-photon process is larger than the corresponding resonant three- and four-photon populations, and it is actually the major factor in the emission

at the cavity peak. This suggests a general expansion of $n_{a,f}$, including all the spurious contributions to n -photon emission from off-resonant, lower- m th-order processes (with $m < n$), so that the filtered purity can be approximated as

$$\pi_n^f \approx \frac{n_a^{(n)}}{n_{1,f}^{(1)} + \sum_{m=2}^n n_a^{(m)}}. \quad (26)$$

Finally, to illustrate the feasibility of our proposal with state-of-the-art systems, we show in Fig. 5 the corresponding contour plots of both π_2 and π_2^f for the range of $(\gamma_a, \gamma_\sigma)$ displayed in Figs. 2(a)–2(b) and include points with several cavity QED experimental parameters (summarized in Table 1), evidencing that many of them already lie within a regime of $\pi_2^f \approx 1$. Note that we have adopted a definition of γ_σ that only considers the decay to free space as the 2LS decoherence source, neglecting, e.g., pure dephasing, which is usually relevant in semiconductor scenarios. In Section 4, however, we consider the impact of these extra decoherence channels on our multiphoton emission.

4. IMPACT OF EXPERIMENTAL LIMITATIONS

Up to now, we have considered the ideal situation, in which the only decoherence sources are both the cavity and 2LS losses; in which the cavity decay generally dominates, $\gamma_a \gg \gamma_\sigma$; and where the distinction between the cavity, laser, and 2LS photons can be made perfectly. Even though this ideal situation can be obtained within circuit QED setups [69–71], in the optical regime some of these requirements are more difficult to achieve.

The goal of this section is to analyze the impact of several experimental imperfections in platforms relevant for the implementation of our proposal in the optical regime, such as semiconductor or atomic cavity QED setups. We focus on the case of two-photon emission, which is the one with more immediate prospects to be experimentally implemented. In particular, we analyze: i) the impact of phonon-induced decoherence in Section A; ii) the effect of detecting coherently scattered photons in the cavity emission in Section B; and finally, iii) the robustness of the multiphoton emission in systems with limited driving and limited cancellation of spontaneous emission, that is, $\gamma_a \approx \gamma_\sigma$, in Section C.

Table 1. Table of State-of-the-Art Parameters in Cavity QED, with Special Emphasis on Semiconductor Samples^a

Reference	$\hbar g$	γ_a/g	γ_σ/g	C
SEMICONDUCTORS				
De Santis <i>et al.</i> (2017) [58]	19 μeV	9.4	0.036	~ 12
Giesz <i>et al.</i> (2016) [59]	21 μeV	8.56	0.028	~ 17
Loo <i>et al.</i> (2012) [60]	33 μeV	2.76	0.6	~ 2
Kim <i>et al.</i> (2014) [49]	63 μeV	2.35	0.01	~ 170
Laucht <i>et al.</i> (2009) [61]	60 μeV	1.6	0.1	~ 25
Fischer <i>et al.</i> (2016) [50]	45 μeV	1.3	~ 0.01 [62]	~ 300
Ota <i>et al.</i> (2011) [52]	51 μeV	0.5	0.016	~ 500
Hennessy <i>et al.</i> (2007) [34]	90 μeV	1.1	~ 0.005	~ 1600
Volz <i>et al.</i> (2012) [63]	141 μeV	0.37	~ 0.006 [64]	~ 1800
Srinivasan <i>et al.</i> (2007) [65]	12 μeV	0.33	0.2	~ 60
Arakawa <i>et al.</i> (2012) [66]	80 μeV	0.3	0.01 [52]	~ 2500
ATOMS				
Hansen <i>et al.</i> (2016) [67]	80 neV	0.2	0.25	~ 80
Birnbaum <i>et al.</i> (2005) [68]	0.14 μeV	0.12	0.071	~ 470

^aThe high cooperativity values shown by semiconductor systems are because we are not considering in the definition the phonon-induced decoherence, which will reduce the effective cooperativity. We will consider its impact in detail in part A of Section 4.

A. Phonon-Induced Decoherence

One of the main problems in semiconductor cavity QED implementations is the decoherence produced by the phonons induced by the lattice vibrations in the solid. It is a well-known fact that phonons in cavity QED systems [72] give rise to two effects. The first one is the so-called pure dephasing mechanism, in which the phonons spoil the coherence of the 2LS without directly affecting the populations. This mechanism can be described in a master equation description through the Lindblad term $\frac{\gamma_\phi}{2} \mathcal{L}_{\sigma^\dagger \sigma}[\rho]$.

Moreover, when the 2LS is also interacting with a cavity mode, the phonons open an extra channel that allows one to exchange excitations incoherently between the cavity and the 2LS. This is the *cavity feeding* mechanism [72–75], described by the following Lindblad terms:

$$\frac{\gamma_{\sigma^\dagger a}}{2} \mathcal{L}_{\sigma^\dagger a}[\rho] + \frac{\gamma_{\sigma a^\dagger}}{2} \mathcal{L}_{\sigma a^\dagger}[\rho], \quad (27)$$

where, following Ref. [72], we estimate the phonon transfer rates to be given by

$$\gamma_{\sigma^\dagger a/\sigma a^\dagger} = 2\langle B \rangle^2 g^2 \Re \left[\int_0^\infty d\tau e^{\pm i\Delta_a \tau} (e^{\phi(\tau)} - 1) \right], \quad (28)$$

where $\langle B \rangle$ is

$$\langle B \rangle = \exp \left[-\frac{1}{2} \int_0^\infty d\omega \frac{J(\omega)}{\omega^2} \coth(\beta \hbar \omega / 2) \right], \quad (29)$$

$\phi(t)$ is

$$\phi(t) = \int_0^\infty d\omega \frac{J(\omega)}{\omega^2} [\coth(\beta \hbar \omega / 2) \cos(\omega t) - i \sin(\omega t)], \quad (30)$$

and $J(\omega)$, the characteristic phonon spectral function, is defined as $J(\omega) = \alpha_p \omega^3 \exp(-\frac{\omega^2}{2\omega_b^2})$. Obviously, the higher the temperature is, the more relevant these mechanisms are. In Fig. 6, we illustrate the impact of these two mechanisms in the two-photon emission as a function of temperature. To do so, we choose a pure dephasing rate proportional to temperature, $\gamma_\phi = AT$, with $A = 1 \mu\text{eV/K}$ [72,76], and set the parameters as $\omega_b = 0.22 \text{ meV}$ and $\alpha_p = 0.18 \text{ meV}^{-2}$, consistently with those provided in Refs. [50,62]. The resulting values for $\gamma_{\sigma^\dagger a}$ and $\gamma_{\sigma a^\dagger}$ as a function of temperature are shown explicitly in Fig. 6(a). In Fig. 6(b) we study the effect of the temperature on $n_{a,f}$, the cavity population emitted at the cavity frequency, in a plot similar to panel (c) of Fig. 2: the filtered emission is shown as a function of Ω and compared with the amount of two-photon population, $n_a^{(2)}$. We observe that for drivings $\Omega/g \gtrsim 20$, the two-photon population still dominates the emission [$n_a^{(2)} \approx n_{a,f}$], even for relatively large temperatures of $T \approx 30 \text{ K}$. The oscillatory behavior stems from the oscillatory dependence of $\gamma_{\sigma^\dagger a/\sigma a^\dagger}$ with Δ_a in Eq. (28), magnified by the logarithmic scale. At smaller driving amplitudes, the extra broadening introduced by phonons increases the emission of spurious single photons, therefore decreasing the importance of the two-photon mechanism.

It is interesting to highlight that even for a temperature of $T = 30 \text{ K}$, the spectral signature of the two-photon processes in $S(\omega)$ remains unambiguous. This remains true even for systems with moderate driving strength, as we show in the contour plot of Fig. 6(c), where we plot the evolution of $S(\omega)$ as a function of the driving amplitude for a fixed $\Delta_a = 5g$ [as in Fig. 1(a)]. There, we observe that apart from the expected broadening of the peaks in $S(\omega)$, and the enhancement of single-photon features, we still observe a well-distinguished peak when Ω is such that

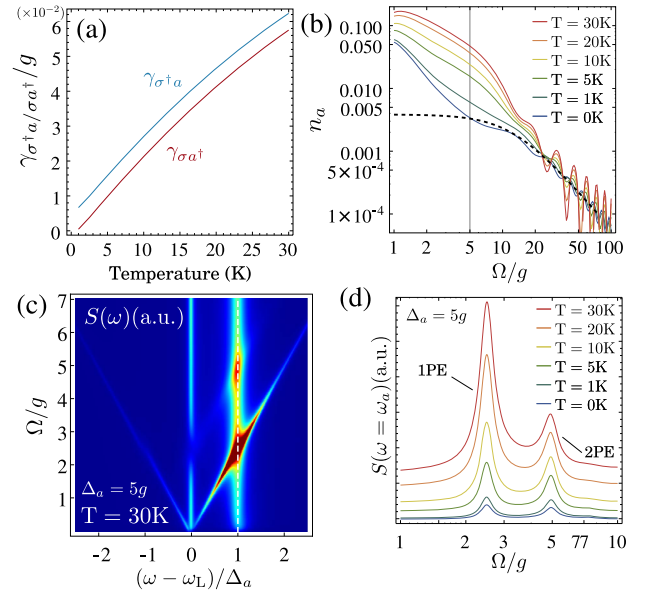


Fig. 6. (a) Calculated rates for the phonon-induced transitions as a function of temperature. (b) Cavity population emitted at the cavity frequency as a function of Ω for a cavity at the two-photon resonance $\Delta_a = \Omega$ and different temperatures. Dashed, black: two-photon population. (c) Spectrum of cavity emission as a function of the amplitude of the driving field for $T = 30 \text{ K}$. $\Delta_a = 5g$. (d) Spectrum at the cavity frequency as a function of driving field amplitude and different temperatures. $\Delta_a = 5g$.

$\Delta_a = \Delta_a^{(2)} = 5g$. To make more evident that phonons do not preclude the observation of two-photon emission features, we finally plot in Fig. 6(d) the value of the cavity spectrum at the cavity frequency $\omega = \omega_a$ as a function of Ω and temperature T and for a fixed $\Delta_a = 5g$. Remarkably, we observe that phonon-induced transitions not only result in an enhancement of single-photon emission expected from the larger overlap with cavity peak, but also enhance the two-photon emission peak. This indicates that unambiguous signatures of two-photon physics can be observed even at high temperatures.

B. Driving via the Cavity Mode: Laser Coherent Back-Scattering

In our model we have assumed that the 2LS can be coherently driven independently of the cavity channel. Though this is certainly a possible configuration, in both semiconductor [49,50] and atom cavity QED setups [67], the most common scenario experimentally is the one where the 2LS is driven coherently through the cavity channel. In order to describe that situation, we replace $\Omega(\sigma + \sigma^\dagger) \rightarrow \Omega(a + a^\dagger)$ in the Hamiltonian of Eq. (1). We can nevertheless come back to the description in terms of 2LS driving that we have used so far by rewriting the cavity operator as $a \rightarrow \alpha + a$, with α a complex number, and setting $\alpha = \Omega/(\Delta_a - i\gamma_a/2)$. This choice cancels the cavity driving terms in the master equation (where now the cavity operator describes the creation of quantum fluctuations on top of the coherent state built by the laser). This finally results in a Hamiltonian with an effective coherent driving in the 2LS given by $\Omega_{\text{eff}}(e^{-i\phi}\sigma + e^{i\phi}\sigma^\dagger)$, with $\phi = \arg(\alpha)$ and $\Omega_{\text{eff}} = |\Omega/(\Delta_a - i\gamma_a/2)|$. This means that all the results obtained so far apply to this case by just replacing Ω by Ω_{eff} .

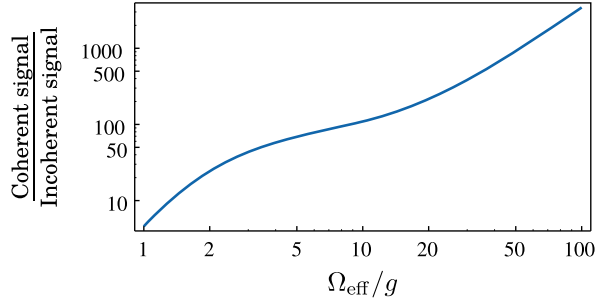


Fig. 7. Ratio between the coherent and incoherent signals at the cavity frequency when the cavity is coherently driven, as a function of the effective driving of the 2LS. In order to describe the situation where the full cavity peak is filtered, the filter linewidth has been taken equal to the cavity linewidth, $\Gamma = \gamma_a$. For each value of the driving, the cavity frequency is tuned to the two-photon resonance, $\Delta_a = \Omega_{\text{eff}}$.

However, this type of driving leads to a potential problem, that is, the presence of coherently scattered light in the cavity spectrum, $S(\omega) = S_I(\omega) + S_C(\omega)$, which obviously spoils the multi-photon response, and which needs to be rejected. The amount of coherently scattered photons $S_C(\omega)$ when we place a filter of linewidth Γ is given by

$$S_C = \frac{\Gamma^2}{2} \frac{|\langle a \rangle|^2}{\Gamma^2/4 + \omega^2}. \quad (31)$$

The ratio $S_C(\omega_a)/S_I(\omega_a)$ dictates what would be the experimental rejection of coherently scattered light required to avoid the laser background to overcome the incoherent signal. In Fig. 7, we plot this ratio as a function of Ω_{eff} in the case of two-photon emission, i.e., $\Delta_a = \Omega_{\text{eff}}$, for a filter linewidth equal to the width of the cavity peak, $\Gamma = \gamma_a$, and a cavity decay rate representative of semiconductor samples, $\gamma_a \approx g$. We see that, even for effective drivings as large as $\Omega_{\text{eff}} \sim 100g$, the ratio between coherent and incoherent scattered signal remains below 10^4 , which can be understood, since in order to achieve two-photon emission the detuning between the cavity and the driving also increases with Ω_{eff} . This shows that, in that case, state-of-the-art rejection ratios of $\sim 10^{-6}$ [77–79] would yield only $\sim 1\%$ of detected photons coming from the coherent signal, and only $\sim 0.01\%$ for drivings of $\Omega_{\text{eff}} \approx 20$, which we have shown in previous sections to be sufficient to achieve regimes of perfect two-photon emission, $\pi_2^f \approx 1$ [80]. The present analysis of the required rejection ratio is also relevant in the context of recent developments that aim to achieve on-chip suppression of the coherent light by self-homodyned techniques [50,81].

C. Limited Driving Amplitude and Limited Cancellation of Spontaneous Emission

Finally, we also explore in more detail how the spectral signatures for multiphoton emission look in the regime of parameters of atomic cavity QED systems [67]. A typical restriction in those systems is that the 2LS spontaneous emission is not suppressed, such that it is $\gamma_\sigma \approx \gamma_a$, but with the advantage of being in the strong nonlinear coupling $g > \gamma_{a,\sigma}$. Another limitation is that the drivings cannot be very large, as it will decrease the trapping lifetime of the atom. In order to illustrate that the two-photon emission signatures are still visible in this regime of parameters, we plot the evolution of $S(\omega)$ as a function of Ω for a fixed

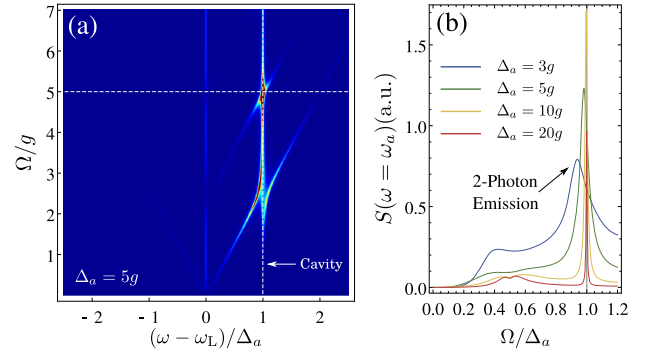


Fig. 8. (a) Cavity spectrum as a function of the driving amplitude Ω for set of parameters typical of atomic cavity QED systems, $\gamma_a = \gamma_\sigma = 0.1g$. The detuning between cavity and 2LS is $\Delta_a = 5g$. (b) Value of the spectrum at the cavity frequency ω_a as a function of the driving amplitude Ω , for four fixed sets of cavity frequencies. A feature indicating two-photon emission appears whenever $\Omega = \Delta_a$, and it appears for driving amplitudes as low as $3g$.

$\Delta_a = 5g$ and a system with $\gamma_a = \gamma_\sigma = 0.1g$. Comparing with Fig. 1(a), we observe that: i) at the single-photon resonance, an anticrossing with the resonant sideband, is present as the system is in the strong nonlinear coupling; ii) more interesting for our paper, there is still a very strong signature when Ω matches the two-photon resonance at $\Omega = \Delta_a$.

Finally, we illustrate the effect of smaller drivings in Fig. 8(b), where we plot the amount of emission at the cavity resonance $S(\omega_a)$ as a function of Ω for several values of Δ_a . For large Δ_a , e.g., $20g$, that corresponds to large drivings, one observes a very sharp peak at the two-photon resonance. As one decreases Δ_a , the height of the peak decreases, and it gets broader. However, even for very small drivings/detunings $\Omega = \Delta_a = 3g$, the two-photon spectral resonance is still observed.

5. CONCLUSIONS AND OUTLOOK

In this work, we have shown how to optimally exploit the mechanism of n -photon emission introduced in Ref. [32], based on a coherently driven 2LS coupled to a cavity mode. In particular, we have provided an analytical understanding of the figures of merit of the emission such as the efficiency rates, purity of n -photon emission, and its spectral distribution in the cavity output field. Thanks to these closed-form expressions, we provide formulas for the optimal driving, Ω , and the emitter's decay rate, γ_σ , to maximize the n -photon emission. More importantly, we identify that the spurious single photons can be filtered out, relaxing in some situations the strong coupling requirement used in the previous proposal, to the more accessible *bad-cavity* regime, and thus opening the possibility of implementing this protocol in a wide variety of platforms. Our results also allow us to foresee the future of this field in systems with parameters still out of reach for most platforms, which we have shown to produce close to 100% three- and four-photon emission with demanding but still realistic parameters. Finally, we analyze the impact of several experimental imperfections, such as phonon-induced decoherence, on the n -photon emission showing how they are within the reach of current experimental technologies in semiconductor and atom cavity QED setups.

In future works, it will be interesting to introduce another controllable decay channel on the 2LS, e.g., another cavity mode,

which allows one to control dynamically the decay rate of γ_σ . With that knob, one can tune the optimal n -photon emission regime or control the temporal separation between the n -photon states. Moreover, by measuring the emission of that channel, one can herald the presence of the n -photon states in the cavity one, as these processes can be shown to be strongly correlated [32]. Other heralding protocols could benefit from exploiting higher-order frequency-resolved correlations in the emission [82]. Further exciting perspectives are the triggered generation of n -photon states with appropriate pulse shaping of $\Omega(t)$, or the study of the interplay of these mechanisms taking into account other spectral densities as the ones appearing in band-edges of waveguide QED setups.

Funding. H2020 European Research Council (ERC) (308136); FP7 People: Marie-Curie Actions (PEOPLE) (625955); Ministerio de Economía y Competitividad (MINECO) (FIS2015-64951-R, MAT2014-53119-C2-1-R); Japan Society for the Promotion of Science (JSPS).

Acknowledgment. The authors thank Kevin Fischer for stimulating discussions. C. S. M. acknowledges a short-term fellowship from the Japan Society for the Promotion of Science (JSPS). F. P. L. acknowledges the POLAFLOW ERC project. E.dV. acknowledges the project (CLAUQUE) and RyC program. C. T. acknowledges financial support from the Spanish MINECO. A. G. T. acknowledges support from Intra-European Marie-Curie Fellowship NanoQuIS.

See Supplement 1 for supporting content.

REFERENCES AND NOTES

1. H. Kimble, "The quantum internet," *Nature* **453**, 1023–1030 (2008).
2. V. Giovannetti, S. Lloyd, and L. Maccone, "Quantum metrology," *Phys. Rev. Lett.* **96**, 010401 (2006).
3. M. D'Angelo, M. V. Chekhova, and Y. Shih, "Two-photon diffraction and quantum lithography," *Phys. Rev. Lett.* **87**, 013602 (2001).
4. J. López Carreño, C. S. Muñoz, D. Sanvitto, E. del Valle, and F. Laussy, "Exciting polaritons with quantum light," *Phys. Rev. Lett.* **115**, 196402 (2015).
5. K. E. Dorfman, F. Schlöwin, and S. Mukamel, "Nonlinear optical signals and spectroscopy with quantum light," *Rev. Mod. Phys.* **88**, 045008 (2016).
6. W. Denk, J. Strickler, and W. Webb, "Two-photon laser scanning fluorescence microscopy," *Science* **248**, 73–76 (1990).
7. N. Horton, D. Wang, C. Kibat, F. Clark, C. Wise, and C. X. C. Schaffer, "In vivo three-photon microscopy of subcortical structures of an intact mouse brain," *Nat. Photonics* **7**, 205–209 (2013).
8. Y. Xu, J. Vučković, R. Lee, O. Painter, A. Scherer, and A. Yariv, "Finite-difference time-domain calculation of spontaneous emission lifetime in a microcavity," *J. Opt. Soc. Am. B* **16**, 465–474 (1999).
9. O. Painter, R. K. Lee, A. Scherer, A. Yariv, J. D. O'Brien, P. D. Dapkus, and I. Kim, "Two-dimensional photonic band-gap defect mode laser," *Science* **284**, 1819–1821 (1999).
10. H. J. Kimble and L. Mandel, "Theory of resonance fluorescence," *Phys. Rev. A* **13**, 2123–2144 (1976).
11. C. Matthiesen, A. N. Vamivakas, and M. Atatüre, "Subnatural linewidth single photons from a quantum dot," *Phys. Rev. Lett.* **108**, 093602 (2012).
12. R. Proux, M. Maragkou, E. Baudin, C. Voisin, P. Roussignol, and C. Diederichs, "Measuring the photon coalescence time window in the continuous-wave regime for resonantly driven semiconductor quantum dots," *Phys. Rev. Lett.* **114**, 067401 (2015).
13. N. Somaschi, V. Giesz, L. D. Santis, J. C. Lored, M. P. Almeida, G. Hornecker, S. L. Portalupi, T. Grange, C. Anton, J. Demory, C. Gomez, I. Sagnes, N. D. Lanzillotti-Kimura, A. Lemaitre, A. Auffeves, A. G. White, L. Lanco, and P. Senellart, "Near-optimal single-photon sources in the solid state," *Nat. Photonics* **10**, 340–345 (2016).
14. M. Arcari, I. Söllner, A. Javadi, S. Lindskov Hansen, S. Mahmoodian, J. Liu, H. Thyrrestrup, E. H. Lee, J. D. Song, S. Stobbe, and P. Lodahl, "Near-unity coupling efficiency of a quantum emitter to a photonic crystal waveguide," *Phys. Rev. Lett.* **113**, 093603 (2014).
15. N. Bruno, A. Martin, T. Guerreiro, B. Sanguinetti, and R. T. Thew, "Pulsed source of spectrally uncorrelated and indistinguishable photons at telecom wavelengths," *Opt. Express* **22**, 17246–17253 (2014).
16. G. Callsen, A. Carmele, G. Hönig, C. Kindel, J. Brunnmeier, M. R. Wagner, E. Stock, J. S. Reparaz, A. Schliwa, S. Reitzenstein, A. Knorr, A. Hoffmann, S. Kako, and Y. Arakawa, "Steering photon statistics in single quantum dots: from one- to two-photon emission," *Phys. Rev. B* **87**, 245314 (2013).
17. A. Dousse, J. Suffczynski, A. Beveratos, O. Krebs, A. Lemaitre, I. Sagnes, J. Bloch, P. Voisin, and P. Senellart, "Ultrabright source of entangled photon pairs," *Nature* **466**, 217–220 (2010).
18. M. Müller, S. Bounouar, K. D. Jöns, M. Glässl, and P. Michler, "On-demand generation of indistinguishable polarization-entangled photon pairs," *Nat. Photonics* **8**, 224–228 (2014).
19. X.-C. Yao, T.-X. Wang, P. Xu, H. Lu, G.-S. Pan, X.-H. Bao, C.-Z. Peng, C.-Y. Lu, Y.-A. Chen, and J.-W. Pan, "Observation of eight-photon entanglement," *Nat. Photonics* **6**, 225–228 (2012).
20. P. Bienias, S. Choi, O. Firstenberg, M. F. Maghrebi, M. Gullans, M. D. Lukin, A. V. Gorshkov, and H. P. Büchler, "Scattering resonances and bound states for strongly interacting rydberg polaritons," *Phys. Rev. A* **90**, 053804 (2014).
21. M. F. Maghrebi, M. J. Gullans, P. Bienias, S. Choi, I. Martin, O. Firstenberg, M. D. Lukin, H. P. Büchler, and A. V. Gorshkov, "Coulomb bound states of strongly interacting photons," *Phys. Rev. Lett.* **115**, 123601 (2015).
22. O. Firstenberg, C. S. Adams, and S. Hofferberth, "Nonlinear quantum optics mediated by Rydberg interactions," *J. Phys. B* **49**, 152003 (2016).
23. A. González-Tudela, V. Paulisch, D. E. Chang, H. J. Kimble, and J. I. Cirac, "Deterministic generation of arbitrary photonic states assisted by dissipation," *Phys. Rev. Lett.* **115**, 163603 (2015).
24. J. S. Douglas, T. Caneva, and D. E. Chang, "Photon molecules in atomic gases trapped near photonic crystal waveguides," *Phys. Rev. X* **6**, 031017 (2016).
25. A. González-Tudela, V. Paulisch, H. J. Kimble, and J. I. Cirac, "Efficient multiphoton generation in waveguide quantum electrodynamics," *Phys. Rev. Lett.* **118**, 213601 (2017).
26. K. Koshino, K. Inomata, T. Yamamoto, and Y. Nakamura, "Implementation of an impedance-matched λ system by dressed-state engineering," *Phys. Rev. Lett.* **111**, 153601 (2013).
27. C. Sánchez-Muñoz, F. P. Laussy, C. Tejedor, and E. del Valle, "Enhanced two-photon emission from a dressed biexciton," *New J. Phys.* **17**, 123021 (2015).
28. Y. Chang, A. González-Tudela, C. S. Muñoz, C. Navarrete-Benlloch, and T. Shi, "Deterministic down-converter and continuous photon-pair source within the bad-cavity limit," *Phys. Rev. Lett.* **117**, 203602 (2016).
29. E. Sánchez-Burillo, L. Martín-Moreno, J. García-Ripoll, and D. Zueco, "Full two-photon down-conversion of a single photon," *Phys. Rev. A* **94**, 053814 (2016).
30. F. Hargart, M. Müller, K. Roy-Choudhury, S. L. Portalupi, C. Schneider, S. Höfling, M. Kamp, S. Hughes, and P. Michler, "Cavity-enhanced simultaneous dressing of quantum dot exciton and biexciton states," *Phys. Rev. B* **93**, 115308 (2016).
31. C. K. Law and J. H. Eberly, "Arbitrary control of a quantum electromagnetic field," *Phys. Rev. Lett.* **76**, 1055–1058 (1996).
32. C. Sanchez Muñoz, E. del Valle, A. G. Tudela, K. Müller, S. Lichtmannecker, M. Kaniber, C. Tejedor, J. Finley, and F. Laussy, "Emitters of N -photon bundles," *Nat. Photonics* **8**, 550–555 (2014).
33. A. Laucht, S. Pütz, T. Günthner, N. Hauke, R. Saive, S. Frédéric, M. Bichler, M.-C. Amann, A. W. Holleitner, M. Kaniber, and J. J. Finley, "A waveguide-coupled on-chip single-photon source," *Phys. Rev. X* **2**, 011014 (2012).
34. K. Hennessy, A. Badolato, M. Winger, D. Gerace, M. Atatüre, S. Gulde, S. Falt, E. L. Hu, and A. Imamoglu, "Quantum nature of a strongly

- coupled single quantum dot-cavity system," *Nature* **445**, 896–899 (2007).
35. P. Lodahl, S. Mahmoodian, and S. Stobbe, "Interfacing single photons and single quantum dots with photonic nanostructures," *Rev. Mod. Phys.* **87**, 347–400 (2015).
 36. M. N. Makhonin, J. E. Dixon, R. J. Coles, B. Royall, I. J. Luxmoore, E. Clarke, M. Hugues, M. S. Skolnick, and A. M. Fox, "Waveguide coupled resonance fluorescence from on-chip quantum emitter," *Nano Lett.* **14**, 6997–7002 (2014).
 37. A. Goban, C.-L. Hung, S.-P. Yu, J. Hood, J. Muniz, J. Lee, M. Martin, A. McClung, K. Choi, D. Chang, O. Painter, and H. Kimble, "Atom-light interactions in photonic crystals," *Nat. Commun.* **5**, 3808 (2014).
 38. J. D. Thompson, T. G. Tiecke, N. P. de Leon, J. Feist, A. V. Akimov, M. Gullans, A. S. Zibrov, V. Vuletic, and M. D. Lukin, "Coupling a single trapped atom to a nanoscale optical cavity," *Science* **340**, 1202–1205 (2013).
 39. B. R. Mollow, "Power spectrum of light scattered by two-level systems," *Phys. Rev.* **188**, 1969–1975 (1969).
 40. S. Haroche and D. Kleppner, "Cavity quantum electrodynamics," *Phys. Today* **42**(1), 24–30 (1989).
 41. R. Miller, T. E. Northup, K. M. Birnbaum, A. Boca, A. D. Boozer, and H. J. Kimble, "Trapped atoms in cavity QED: coupling quantized light and matter," *J. Phys. B* **38**, S551 (2005).
 42. F. P. Laussy, E. del Valle, M. Schrapp, A. Laucht, and J. J. Finley, "Climbing the Jaynes-Cummings ladder by photon counting," *J. Nanophoton.* **6**, 061803 (2012).
 43. C. N. Cohen-Tannoudji and S. Reynaud, "Dressed-atom description of resonance fluorescence and absorption spectra of a multi-level atom in an intense laser beam," *J. Phys. B At. Mol. Opt. Phys.* **10**, 345–363 (1977).
 44. E. del Valle, A. Gonzalez-Tudela, F. P. Laussy, C. Tejedor, and M. J. Hartmann, "Theory of frequency-filtered and time-resolved N-photon correlations," *Phys. Rev. Lett.* **109**, 183601 (2012).
 45. A. Gonzalez-Tudela, F. P. Laussy, C. Tejedor, M. J. Hartmann, and E. del Valle, "Two-photon spectra of quantum emitters," *New J. Phys.* **15**, 033036 (2013).
 46. M. Peiris, B. Petrak, K. Konthasinghe, Y. Yu, Z. C. Niu, and A. Muller, "Two-color photon correlations of the light scattered by a quantum dot," *Phys. Rev. B* **91**, 195125 (2015).
 47. M. Peiris, K. Konthasinghe, and A. Muller, "Franson interference generated by a two-level system," *Phys. Rev. Lett.* **118**, 030501 (2017).
 48. C. Sánchez-Muñoz, E. del Valle, C. Tejedor, and F. P. Laussy, "Violation of classical inequalities by photon frequency filtering," *Phys. Rev. A* **90**, 052111(2014).
 49. H. Kim, T. C. Shen, K. Roy-Choudhury, G. S. Solomon, and E. Waks, "Resonant interactions between a Mollow triplet sideband and a strongly coupled cavity," *Phys. Rev. Lett.* **113**, 027403 (2014).
 50. K. A. Fischer, K. Müller, A. Rundquist, T. Sarmiento, A. Y. Piggott, Y. Kelaita, C. Dory, and K. G. L. J. Vuckovic, "Self-homodyne measurement of a dynamic Mollow triplet in the solid state," *Nat. Photonics* **10**, 163–166 (2016).
 51. A. Ulhaq, S. Weiler, S. M. Ulrich, R. Roßbach, M. Jetter, and P. Michler, "Cascaded single-photon emission from the Mollow triplet sidebands of a quantum dot," *Nat. Photonics* **6**, 238–242 (2012).
 52. Y. Ota, S. Iwamoto, N. Kumagai, and Y. Arakawa, "Spontaneous two-photon emission from a single quantum dot," *Phys. Rev. Lett.* **107**, 233602 (2011).
 53. Note that the definition of π_n introduced in Ref. [32] differs slightly with the one used here. In that work, it was defined as $\pi_n = \frac{\lambda_n}{\lambda_n + \lambda_1}$, where λ_n are fitted from photon counting distributions and correspond to $\lambda_n = \gamma_a n_a^{(n)} / n$. The comparison was made adopting the definition used in this text and defining $\pi_n = \frac{\lambda_n/n}{\lambda_n/n + \lambda_1}$.
 54. A. González-Tudela, V. Paulisch, D. E. Chang, H. J. Kimble, and J. I. Cirac, "Deterministic generation of arbitrary photonic states assisted by dissipation," *Phys. Rev. Lett.* **115**, 163603 (2015).
 55. E. del Valle, "Distilling one, two and entangled pairs of photons from a quantum dot with cavity QED effects and spectral filtering," *New J. Phys.* **15**, 025019 (2013).
 56. E. del Valle and F. P. Laussy, "Regimes of strong light-matter coupling under incoherent excitation," *Phys. Rev. A* **84**, 043816 (2011).
 57. E. del Valle, *Microcavity Quantum Electrodynamics* (VDM Verlag, 2010).
 58. L. de Santis, C. Antón, B. Reznichenko, N. Somaschi, G. Coppola, J. Senellart, C. Gómez, A. Lemaître, I. Sagnes, A. G. White, L. Lanco, A. Auffeves, and P. Senellart, "A solid-state single-photon filter," *Nat. Nanotechnol.* **12**, 663 (2017).
 59. V. Giesz, N. Somaschi, G. Hornecker, T. Grange, B. Reznichenko, L. D. Santis, J. Demory, C. Gomez, I. Sagnes, A. Lemaître, O. Krebs, N. D. Lanzillotti-Kimura, L. Lanco, A. Auffeves, and P. Senellart, "Coherent manipulation of a solid-state artificial atom with few photons," *Nat. Commun.* **7**, 11986 (2016).
 60. V. Loo, C. Arnold, O. Gazzano, A. Lemaître, I. Sagnes, O. Krebs, P. Voisin, P. Senellart, and L. Lanco, "Optical nonlinearity for few-photon pulses on a quantum dot-pillar cavity device," *Phys. Rev. Lett.* **109**, 166806 (2012).
 61. A. Laucht, F. Hofbauer, N. Hauke, J. Angele, S. Stobbe, M. Kaniber, G. Böhm, P. Lodahl, M.-C. Amann, and J. J. Finley, "Electrical control of spontaneous emission and strong coupling for a single quantum dot," *New J. Phys.* **11**, 023034 (2009).
 62. K. Müller, K. A. Fischer, A. Rundquist, C. Dory, K. G. Lagoudakis, T. Sarmiento, Y. A. Kelaita, V. Borish, and J. Vučković, "Ultrafast polariton-phonon dynamics of strongly coupled quantum dot-nanocavity systems," *Phys. Rev. X* **5**, 031006 (2015).
 63. T. Volz, A. Reinhard, M. Winger, A. Badolato, D. J. Hennessy, E. L. Hu, and A. Imamoglu, "Ultrafast all-optical switching by single photons," *Nat. Photonics* **6**, 605–611 (2012).
 64. Value not provided in the reference. We assumed the typical value of the QD lifetime in a photonic bandgap of ~ 5 ns.
 65. K. Srinivasan and O. Painter, "Linear and nonlinear optical spectroscopy of a strongly coupled microdisk-quantum dot system," *Nature* **450**, 862–865 (2007).
 66. Y. Arakawa, S. Iwamoto, M. Nomura, A. Tandraechanurat, and Y. Ota, "Cavity quantum electrodynamics and lasing oscillation in single quantum dot-photonic crystal nanocavity coupled systems," *IEEE J. Sel. Top. Quantum Electron.* **18**, 1818–1829 (2012).
 67. C. Hamsen, K. N. Tolazzi, T. Wilk, and G. Remppe, "Two-photon blockade in an atom-driven cavity QED system," *Phys. Rev. Lett.* **118**, 133604 (2017).
 68. K. Birnbaum, A. Boca, R. Miller, A. Boozer, T. Northup, and H. Kimble, "Photon blockade in an optical cavity with one trapped atom," *Nature* **436**, 87–90 (2005).
 69. A. A. Houck, H. E. Türeci, and J. Koch, "On-chip quantum simulation with superconducting circuits," *Nat. Phys.* **8**, 292–299 (2012).
 70. J. You and F. Nori, "Superconducting circuits and quantum information," *Phys. Today* **58**(11), 42–47 (2005).
 71. X. Gu, A. F. Kockum, A. Miranowicz, Y.-X. Liu, and F. Nori, "Microwave photonics with superconducting quantum circuits," *Phys. Rep.* **718–719**, 1–102 (2017).
 72. C. Roy and S. Hughes, "Influence of electron-acoustic-phonon scattering on intensity power broadening in a coherently driven quantum-dot-cavity system," *Phys. Rev. X* **1**, 021009 (2011).
 73. U. Hohenester, A. Laucht, M. Kaniber, N. Hauke, A. Neumann, A. Mohtashami, M. Seliger, M. Bichler, and J. J. Finley, "Phonon-assisted transitions from quantum dot excitons to cavity photons," *Phys. Rev. B* **80**, 201311(R) (2009).
 74. U. Hohenester, "Cavity quantum electrodynamics with semiconductor quantum dots: role of phonon-assisted cavity feeding," *Phys. Rev. B* **81**, 155303 (2010).
 75. K. Müller, A. Rundquist, K. A. Fischer, T. Sarmiento, K. G. Lagoudakis, Y. A. Kelaita, C. S. Muñoz, E. del Valle, F. P. Laussy, and J. Vučković, "Coherent generation of nonclassical light on chip via detuned photon blockade," *Phys. Rev. Lett.* **114**, 233601 (2015).
 76. M. Bayer and A. Forchel, "Temperature dependence of the exciton homogeneous linewidth in $\text{In}_{0.60}\text{Ga}_{0.40}\text{As}$ self-assembled quantum dots," *Phys. Rev. B* **65**, 041308(R) (2002).
 77. A. V. Kuhlmann, J. Houel, D. Brunner, A. Ludwig, D. Reuter, A. D. Wieck, and R. J. Warburton, "A dark-field microscope for background-free detection of resonance fluorescence from single semiconductor quantum dots operating in a set-and-forget mode," *Rev. Sci. Instrum.* **84**, 073905 (2013).
 78. E. B. Flagg, A. Muller, J. W. Robertson, S. Founta, D. G. Deppe, M. Xiao, W. Ma, G. J. Salamo, and C. K. Shih, "Resonantly driven coherent oscillations in a solid-state quantum emitter," *Nat. Phys.* **5**, 203–207 (2009).
 79. Y.-M. He, Y. He, Y.-J. Wei, D. Wu, M. Atatüre, C. Schneider, S. Höfling, M. Kamp, C.-Y. Lu, and J.-W. Pan, "On-demand semiconductor

- single-photon source with near-unity indistinguishability,” *Nat. Nanotechnol.* **8**, 213–217 (2013).
80. We note that the predicted π_2^f has been obtained by assuming one can perfectly filter the two-photon contribution with respect to the single-photon one. To give a more accurate quantitative estimation, one needs to take into account a realistic filter in the calculation.
81. K. A. Fischer, Y. A. Kelaita, N. V. Saprà, C. Dory, K. G. Lagoudakis, K. Müller, and J. Vučković, “On-chip architecture for self-homodyned nonclassical light,” *Phys. Rev. Appl.* **7**, 044002 (2017).
82. J. C. L. Carreño, E. del Valle, and F. P. Laussy, “Photon correlations from the Mollow triplet,” *Laser Photon. Rev.* **11**, 1700090 (2017).